DOI: 10.1002/ange.201005274

Transition-Metal Hydrides

Acid–Base Interaction between Transition-Metal Hydrides: Dihydrogen Bonding and Dihydrogen Evolution**

Vladislava A. Levina, Andrea Rossin, Natalia V. Belkova,* Michele R. Chierotti, Lina M. Epstein, Oleg A. Filippov, Roberto Gobetto, Luca Gonsalvi, Agustí Lledós, Elena S. Shubina,* Fabrizio Zanobini, and Maurizio Peruzzini**

Dedicated to Professor Ivano Bertini on the occasion of his 70th birthday

Unconventional hydrogen bonding that involves transition-metal complexes has attracted considerable attention and several efforts have been made to unravel and rationalize the many conceivable interactions.[1] Core transition metals are able to accept a hydrogen bond through their d-electron lone pairs, thus forming M···HA hydrogen bonds,[2] whereas hydride ligands that possess a partial negative charge are unusual proton-accepting sites that form a dihydrogen bond (DHB), $M\text{-}H^{\delta-}\cdots{}^{\delta+}HA$.[1] The simultaneous presence of both types of bonds was also observed.[3] On the other hand, the reactivity of transition-metal hydrides as proton source is also well appreciated,[4] and hydrogen bonds of the $M\text{-}H^{\delta+}\cdots B$ type (B = organic base) were recently pointed out for neutral transition-metal hydrides.[5] However, DHB interactions where transition metal hydride complexes serve as both proton acceptor and proton donor in a hydrogen bond have not been described to date, although dihydrogen evolution was observed when "hydridic" and "acidic" hydride complexes such as $[OsH_2(PMePh_2)_4]/[CpM(H)(CO)_3]$ system ($Cp = \eta^5\text{-}C_5H_5^-$, M = Mo, W) were allowed to react.[6]

To further investigate this unconventional acid–base interaction, we report herein on the reaction of the stable electron-rich nickel(II) pincer hydride $[(^{tBu}PCP)Ni(H)]$ (**1**) ($^{tBu}PCP = 2,6\text{-}C_6H_3(CH_2PtBu_2)_2$)[7] with the acidic tungsten(II) complex $[CpW(H)(CO)_3]$ (**2**).[5,8] The proton-accepting properties of **1** were first assessed by studying its interaction with excess CF_3CH_2OH (TFE) in $[D_8]$toluene by variable temperature (VT) IR and NMR measurements. The experiments clearly highlighted the dihydrogen bond formation,[9] with a reaction enthalpy $\Delta H°$ of $-2.5\ \text{kcal mol}^{-1}$ and a basicity factor $E_j = 1.06$.[2a,b] Evolution of H_2 was observed with a strong acid such as HBF_4.

Mixing equimolar amounts of **1** and **2** in carefully degassed THF at 273 K under a nitrogen atmosphere led to a dark-orange solution, from which a reddish-orange crystalline material precipitated on slowly raising the temperature to 298 K, accompanied by H_2 evolution. Replacing **1** with $[(^{tBu}PCP)Ni(D)]$ or **2** with $[CpW(D)(CO)_3]$ led to HD formation ($\delta_H = 4.56$ ppm, t, $^1J_{H\text{-}D} = 42.5$ Hz). Single crystal X-ray diffraction analysis revealed that the final product is the bimetallic ion pair $[CpW(CO)_2(\mu\text{-}\kappa,C{:}\kappa,O\text{-}CO)\cdots Ni(^{tBu}PCP)]$ (**3**, Figure 1 and Tables S1, S2 in the Supporting Information).[10]

The most relevant structural feature of **3** is the presence of one carbonyl ligand that bridges the two metal centers in a rather unconventional "isocarbonylic" mode.[11] The slightly

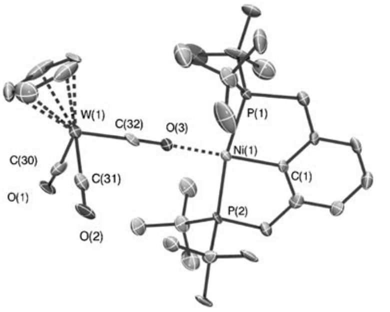

Figure 1. X-ray crystal structure of **3**. Hydrogen atoms on the ligands are omitted for clarity. Thermal ellipsoids set at 40% probability.

---

[*] Dr. A. Rossin, Dr. L. Gonsalvi, Dipl.-Chem. F. Zanobini, Dr. M. Peruzzini
Consiglio Nazionale delle Ricerche (CNR)
Istituto di Chimica dei Composti Organometallici (ICCOM)
via Madonna del Piano 10, 50019 Sesto Fiorentino (Italy)
Fax: (+39) 0555-225-203
E-mail: andrea.rossin@iccom.cnr.it
maurizio.peruzzini@iccom.cnr.it
Homepage: http://www.iccom.cnr.it

Prof. A. Lledós
Universitat Autònoma de Barcelona (UAB)
Departament de Química, Edifici Cn
Bellaterra (Barcelona) (Spain)

V. A. Levina, Dr. N. V. Belkova, Prof. L. M. Epstein, Dr. O. A. Filippov, Prof. E. S. Shubina
A.N. Nesmeyanov Institute of Organoelement Compounds Russian Academy of Sciences, Vavilov str. 28
119991 Moscow (Russia)
E-mail: nataliabelk@ineos.ac.ru
shu@ineos.ac.ru

Dr. M. R. Chierotti, Prof. R. Gobetto
Dipartimento di Chimica I.F.M., Università di Torino, Torino (Italy)

[**] The authors thank "Firenze Hydrolab", a project sponsored by Ente Cassa di Risparmio di Firenze (ECRF), the PIRODE project by MATTM (Rome), the Russian Foundation for Basic Research (RFBR, project 11-03-01210), and the CNR-RAS bilateral agreement for supporting this research. A.R. would like to thank the Centre de Supercomputació de Catalunya (CESCA) for providing additional computational resources. A.L. thanks the Spanish MICINN (projects CTQ2008-06866-C02-01 and CSD2007-00006). O.F. acknowledges the Russian Federation President grant (MK-314.2010.3)

Supporting information for this article is available on the WWW under http://dx.doi.org/10.1002/anie.201005274.

longer C–O bond with respect to the terminal bonds (1.198(2) versus 1.153(2) Å, respectively), evidences simultaneous electron back-donation from both metal ions. The terminal W–CO bonds (1.955(1) and 1.918(2) Å, respectively) are longer than the bridging bond (1.905(1) Å), thus suggesting a significant dipole from W to Ni. The Ni···O distance (1.972(9) Å) is much longer than that reported for other [(^{iPr}PCP)Ni-OR] (R = H, Me) complexes.[12] The almost linear arrangement of the W-C-O-Ni atoms is evidenced by the bond angle of 160° at the oxygen atom. In keeping with the solid-state structure, three distinct resonances for the CO group at $\delta = 224.0$, 229.0, and 239.4 ppm appear in the ^{13}C CPMAS NMR spectrum (see Figure S1 in the Supporting Information), whereas the ^{13}C NMR spectrum of **3** in [D$_3$]CH$_3$NO$_2$ shows only one carbonyl signal at $\delta = 224.10$ ppm.

By monitoring the process by multinuclear VT NMR and VT IR spectroscopy in the 190–298 K temperature range, strong experimental evidence for the formation of a **1**···**2** adduct preceding the H$_2$ elimination that yields **3** is provided. Thus, in the presence of a nearly equimolar amount of **2**, IR spectra in THF at 190 K showed a slight increase of the ν_{NiH} band intensity (see Figure S2) as expected for dihydrogen bond formation. The appearance of a new high-frequency band at 1750 cm^{-1} was observed in the presence of a 4–10-fold excess of **2** in toluene (see Figure S3). The δ_{NiH} signal shifts toward lower frequencies by only 0.04 ppm in the presence of **2** (4 equivalents, [D$_8$]toluene). VT proton spin–lattice relaxation times T_1 of **1** and **1**···**2** hydride resonances were recorded in [D$_8$]THF (Figure S4). In the measured temperature range, T_1 values for the **1**···**2** adduct are shorter than those observed for **1** (see Table S3), which is due to the presence of the additional dipolar contribution consistent with the formation of a NiH···HW unconventional hydrogen bond. At higher temperature, the resonances caused by **1** and **2** started disappearing while **3** formed together with molecular hydrogen (Scheme 1).

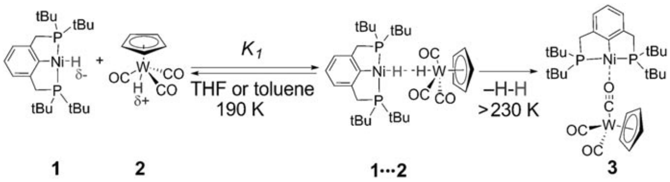

1 **2** **1···2** **3**

Scheme 1. Reaction between metal hydrides **1** and **2**.

IR spectra recorded for a mixture of **1** and a 1.3-fold excess of **2** in both THF and toluene at 190 K (Figure S5–S6) clearly indicated the presence of yet another intermediate with CO absorption signals at 1889 and 1770 cm^{-1}, similar to the ν_{CO} shown by the [CpW(CO)$_3$]$^-$ anion.[13] The same bands were observed in the experiment with [D$_1$]-**1**. These bands are tentatively ascribed to the proton-transfer product **5** (see below) and disappear gradually upon warming. New ν_{CO} bands appear already at 230 K (at 1666, 1824, and a shoulder at 1906 cm^{-1}; Figure S5–S7), thus matching those found in the solid state (KBr) spectrum of **3**. Monitoring the reaction kinetics at room temperature (Figure S7) gave the second order rate constant $k_{obs} = (6.5 \pm 0.1)\,10^{-3}\,\mathrm{M\,s^{-1}}$ which leads to $\Delta G^{\ddagger} = 20.4\,\mathrm{kcal\,mol^{-1}}$ in THF. The reaction mechanism resembles that found for the protonation of basic tungsten hydrides,[14] with the reaction rate expressed by Equation (1)[13] and the observed rate constant $k_{obs} = K_1k_2$, where

$$\frac{-\mathrm{d}[\mathbf{1}]}{\mathrm{d}t} = k'_{obs}[\mathbf{1}] = \frac{k_2k_3}{k_{-2}+k_3}\frac{K_1[\mathbf{2}]}{1+K_1[\mathbf{2}]}[\mathbf{1}] \approx k_2K_1[\mathbf{2}][\mathbf{1}] \qquad (1)$$

k_2 is the rate constant for the proton-transfer step (transformation **1**···**2** to **5**).

Complex **3** dissociates in more polar acetonitrile to give a light yellow solution of the saltlike adduct [(^{tBu}PCP)Ni-(MeCN)]$^+$[CpW(CO)$_3$]$^-$ (**4**) that comprises a square-planar nickel(II) cation binding one MeCN molecule and the piano stool tungsten(II) anion (Figure 2 and Tables S4, S5).

The reaction profile of the H$_2$ evolution has been examined by DFT calculations at the M06 level carried out on the real system and by evaluating the total energies in THF (polarizable continuum model (PCM), Figure 3). An initial intermediate (**1**···**2**) was found, in which the two complexes interact through their hydrides and one cyclopentadienyl

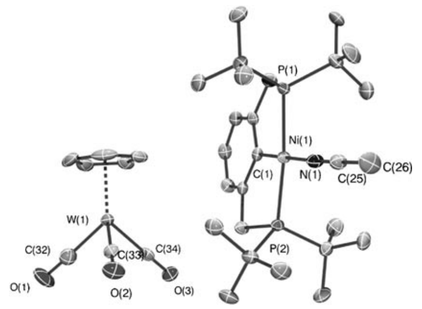

Figure 2. X-ray crystal structure of **4**. Hydrogen atoms on the ligands are omitted for clarity. Thermal ellipsoids set at 40% probability.

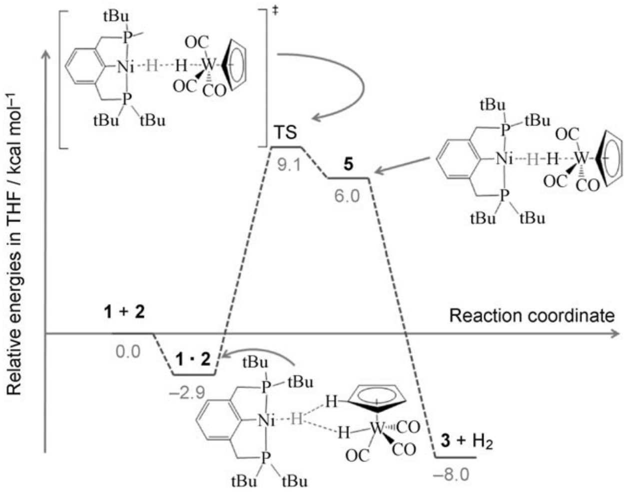

Figure 3. Energy versus reaction coordinate profile for the transformation **1** + **2** → **3** + H$_2$ (THF, PCM). (For the optimized geometries of the various complexes, see Figure S8–S12 and Table S7 in the Supporting Information.)

C–H bond (Figure S8). An atoms-in-molecules (AIM) analysis revealed two (3, −1) critical points between the Ni–H and both C–H and W–H bonds of **2** (Figure S9, Table S6). The interaction energies calculated for each H···H contact are −3.5 and −1.7 kcal mol^{-1}, respectively, which is consistent with the observed shorter contact to the C–H compared to the W–H proton. Despite the stronger Ni–H interaction with the C–H proton, which is most likely caused by the steric hindrance of the bulky *tert*-butyl groups, the most productive interaction in terms of subsequent proton transfer is that with W–H. This result is due to the easier polarization and heterolytic splitting of M–H bonds in comparison to C–H bonds.[15] A transition state (TS) was found, at 12.0 kcal mol^{-1} from the starting geometry (Figure S10). This structure can also be viewed as containing a "bridging nonclassical dihydrogen ligand", judging from the calculated Ni–H, H–H, and H–W distances (1.71, 1.03, and 2.14 Å, respectively). The (elongated) H_2 molecule connects the two metal centers in a quite unusual $\mu,\eta^{1:1}$ end-on mode.[16] Interestingly, a similar structure has been recently calculated in the transition state for the heterolytic H_2 splitting by frustrated Lewis pairs.[17] The late transition-state structure evolves along the intrinsic reaction coordinate (IRC) path towards a "true" proton-transfer product **5**, which is very close in energy (ΔE(TS-**5**) = 3.1 kcal mol^{-1}) and has a very similar geometry to the TS (Figure S11). The experimental difficulty in the isolation of such an elusive dihydrogen intermediate is probably due to the rather flat energy surface around the TS and **5**. From **5**, facile H_2 loss produces **3** as the final thermodynamically stable species (Figure S12, ΔE(**1**···**2**||**3**+H_2) = −5.1 kcal mol^{-1}). Calculations with Grimme's B97D functional gave the same pathway for the **1** + **2** → **3** + H_2 transformation, with very similar structures along the reaction coordinate (see Figure S13–S17).

In conclusion, on the basis of combined crystallographic, spectroscopic (solid state and solution VT NMR and VT IR), and DFT analysis we have collected a large body of evidence for the first example of a DHB adduct between two transition-metal hydrides with opposite polarities; the adduct precedes proton transfer and H_2 evolution. The proton-transfer process proceeds via several intermediates that have been detected and/or computed. Among them, the most remarkable structure is the $\mu,\eta^{1:1}$-H_2 species **5**, which features an end-on coordination mode between the two transition metals. Further studies on the mutual reactivity of acidic and basic transition-metal hydrides are currently underway to highlight the possible role of these unusual interactions in either molecular recognition or bimetallic catalysis involving transition-metal hydrides.

Experimental Section

[CpW(CO)$_2$(μ-κ,*C*:κ,*O*-CO)···Ni($^{t\mathrm{Bu}}$PCP)] **3**: In a typical experiment, **1** (0.15 g, 0.33 mmol) was dissolved in THF (20 mL). The resulting light-yellow solution was cooled to 273 K in an ice bath. **2** (0.16 g, 0.5 mmol, 1.5 equiv) was then added; no color change was observed immediately after the addition. The mixture was stirred for 20 min, and the color slowly turned orange. Subsequently, the temperature was raised to 298 K, and the resulting dark-orange solution was concentrated by evaporation of the solvent under a nitrogen stream to approximately 10 mL. At this point, a crystalline orange solid started to precipitate from the solution. The Schlenk tube was then closed and left to stand under nitrogen over 3 days. Subsequently, the supernatant was filtered off and the needlelike orange crystals were washed with small portions of THF (2 × 5 mL) and dried under nitrogen. Yield: 90 %. IR (KBr): $\tilde{\nu}$(CO) = 1906 (s), 1824 (s), 1666 cm^{-1} (s); ^{1}H NMR (300 MHz, CD_3NO_2, 298 K): δ = 7.26 (m, 3 H; Ar*H*), 5.16 (s, 5 H; Cp), 3.87 (s (br), 4 H; ArC*H*$_2$), 1.52 ppm (virtual triplet (vt), $^*J_{\mathrm{H\text{-}P}}$ = 6.6 Hz, 36 H; C*H*$_3$); ^{13}C NMR (100 MHz, CD_3NO_2, 298 K): δ = 224.1 (*C*O), 163.7 (t, $^2J_{C\text{-}P}$ = 14.9 Hz; $C_{ar\text{-}ipso}$), 151.4 (t, $^2J_{C\text{-}P}$ = 9.7 Hz; $C_{ar\text{-}o}$), 127.2 (s; $C_{ar\text{-}p}$), 120.5 (t, $^3J_{C\text{-}P}$ = 9.7 Hz; $C_{ar\text{-}m}$), 82.3 (s; Cp), 34.1 (vt, $^*J_{\mathrm{C\text{-}P}}$ = 9.0 Hz; P*C*H$_2$), 32.1 (vt, $^*J_{C\text{-}P}$ = 14.2 Hz; P*C*(CH$_3$)$_3$), 26.0 ppm (s; *C*H$_3$); ^{31}P NMR (121.49 MHz, CD_3NO_2, 298 K): δ = 105.7 ppm; elemental analysis calcd for $C_{32}H_{48}NiO_3P_2W$ (785.20): C 48.95, H 6.16; found: C 48.86, H 6.20.

[($^{t\mathrm{Bu}}$PCP)Ni(MeCN)]$^+$[CpW(CO)$_3$]$^-$ **4**: **3** (0.1 g) was dissolved in acetonitrile (5 mL), and a pale yellow solution was obtained. Addition of acetone (ca. 15 mL) followed by concentration of the resulting mixture by evaporation of the solvent with a nitrogen stream led to precipitation of **4** as a pale yellow solid. The supernatant was filtered off, the residue was washed with fresh *n*-pentane (2 × 5 mL) and finally dried in vacuo for 30 min. Crystals suitable for X-ray diffraction analysis were obtained from crystallization of the crude solid from a diluted acetone/*n*-hexane solution. Yield: 92 %. IR (KBr): $\tilde{\nu}$(CO) = 1920 (m), 1887 (s), 1780 cm^{-1} (s); ^{1}H NMR (300 MHz, [D$_6$]acetone, 298 K): δ = 6.92 (m, 3 H; Ar*H*), 5.09 (s, 5 H; Cp), 3.35 (vt, $^*J_{\mathrm{H\text{-}P}}$ = 4.2 Hz, 4 H; ArC*H*$_2$), 1.75 (s, 3 H; C*H*$_3$CN), 1.39 ppm (vt, $^*J_{\mathrm{H\text{-}P}}$ = 6.9 Hz, 36 H; C*H*$_3$); ^{13}C NMR (75 MHz, [D$_6$]acetone, 298 K): δ = 225.7 (s, *C*O), 153.4 (vt, $^2J_{\mathrm{C\text{-}P}}$ = 11.4 Hz; $C_{ar\text{-}ipso}$), 135.2 (s, $C_{ar\text{-}m}$), 126.9 (s; $C_{ar\text{-}p}$), 122.4 (vt, $^2J_{C\text{-}P}$ = 9.0 Hz; $C_{ar\text{-}o}$), 83.8 (s; Cp), 68.3 (*C*H$_3$CN, s), 53.8 (CH$_3$*C*N, t, $^3J_{C\text{-}P}$ = 19.4 Hz), 34.9 (P*C*H$_2$, vt, $^*J_{C\text{-}P}$ = 7.6 Hz), 32.2 ppm (P*C*(CH$_3$)$_3$, vt, $^*J_{C\text{-}P}$ = 13.5 Hz); ^{31}P{^{1}H} NMR (121.49 MHz, [D$_6$]acetone, 298 K): δ = 80.0 ppm; elemental analysis calcd for $C_{34}H_{51}NNiO_3P_2W$ (826.26): C 49.42, H 6.22, N 1.70; found: C 49.30, H 6.36, N 1.61.

General experimental information, details of the synthesis of [D$_1$]-**1**, and of the crystal-structure determinations of **3** and **4** are provided in the Supporting Information, which also includes ^{13}C CPMAS NMR and VT IR spectra, as well as the computational methodology that describes the DFT functional/basis set used and the optimized Cartesian coordinates of the M06-calculated molecules.

Received: August 24, 2010
Revised: November 18, 2010

Keywords: dihydrogen bonding · hydrogen · nickel · transition-metal hydrides · tungsten

---

[1] a) M. Besora, A. Lledós, F. Maseras, *Chem. Soc. Rev.* **2009**, *38*, 957–966; b) N. V. Belkova, E. S. Shubina, L. M. Epstein, *Acc. Chem. Res.* **2005**, *38*, 624–631; c) M. Peruzzini, R. Poli, *Recent Advances in Hydride Chemistry*, Elsevier SA, Amsterdam, NL, **2001**.

[2] a) L. M. Epstein, E. S. Shubina, *Coord. Chem. Rev.* **2002**, *231*, 165–181; b) E. S. Shubina, N. V. Belkova, L. M. Epstein, *J. Organomet. Chem.* **1997**, *536–537*, 17–29; c) L. Brammer, *Dalton Trans.* **2003**, 3145–3157.

[3] a) P. A. Dub, O. A. Filippov, G. A. Silantyev, N. V. Belkova, J.-C. Daran, L. M. Epstein, R. Poli, E. S. Shubina, *Eur. J. Inorg. Chem.* **2010**, 1489–1500; b) N. V. Belkova, M. Besora, M. Baya, P. A. Dub, L. M. Epstein, A. Lledós, R. Poli, P. O. Revin, E. S. Shubina, *Chem. Eur. J.* **2008**, *14*, 9921–9934; c) N. V. Belkova, P. O. Revin, M. Besora, M. Baya, L. M. Epstein, A. Lledós, R. Poli, E. S. Shubina, E. V. Vorontsov, *Eur. J. Inorg. Chem.* **2006**, 2192–2209; d) N. V. Belkova, E. Collange, P. Dub, L. M.

Epstein, D. A. Lemenovskii, A. Lledós, O. Maresca, F. Maseras, R. Poli, P. O. Revin, E. S. Shubina, E. V. Vorontsov, *Chem. Eur. J.* **2005**, *11*, 873 – 888.

[4] S. S. Kristjansdottir, J. R. Norton in *Transition Metal Hydrides* (Ed.: A. Dedieu), VCH, New York, **1991**, pp. 309 – 357.

[5] N. V. Belkova, E. I. Gutsul, O. A. Filippov, V. Levina, D. A. Valyaev, L. M. Epstein, A. Lledós, E. S. Shubina, *J. Am. Chem. Soc.* **2006**, *128*, 3486 – 3487.

[6] K. Abdur-Rashid, T. P. Fong, B. Greaves, D. G. Gusev, J. G. Hinman, S. E. Landau, A. J. Lough, R. H. Morris, *J. Am. Chem. Soc.* **2000**, *122*, 9155 – 9171.

[7] a) B. J. Boro, E. N. Duesler, K. I. Goldberg, R. A. Kemp, *Inorg. Chem.* **2009**, *48*, 5081 – 5087; b) C. J. Moulton, B. L. Shaw, *J. Chem. Soc. Dalton Trans.* **1976**, 1020 – 1024.

[8] R. P. L. Burchell, P. Sirsch, A. Decken, G. S. McGrady, *Dalton Trans.* **2009**, 5851 – 5857.

[9] In the presence of a fivefold TFE excess the NiH resonance of **1** ($\delta = -9.77$ ppm at 220 K) shifts to higher field ($\Delta\delta = -0.25$) and its relaxation time $T_{1\text{min}}$ shortens from 583 ms (210 K) to 244 ms (220 K). IR spectra exhibit a lower frequency shift of the ν_{OH} band of the alcohol, thus evidencing the hydrogen bond formation. The values of (-2.5 ± 0.2) kcal mol^{-1} for $\Delta H°$ and (-4.3 ± 0.8) e.u. for $\Delta S°$ were calculated from the temperature dependence of the DHB formation constant.[1b,2a] The intensity of the ν_{NiH} band at 1739 cm^{-1} decreases in the presence of TFE while a high-frequency shoulder appears at 1770 cm^{-1} at 190 K.

[10] The reaction is not reversible: when a CD_3NO_2 solution of **3** was pressurized with H_2 at 30 bar for 18 hours at room temperature, no reaction was observed; subsequent heating at 60 °C for 2 hours generated unknown decomposition products. No trace of either **1** or **2** was detected in the sample.

[11] Few other crystallographically characterized examples of "isocarbonylic" (μ-κ,C:κ,O-CO) bridges between two metal centres are available; for examples, see: a) S. T. Liddle, B. M. Gardner, *J. Organomet. Chem.* **2009**, *694*, 1581 – 1585 (Y-Cr); b) P. V. Poplaukhin, X. Chen, E. A. Meyers, S. G. Shore, *Inorg. Chem.* **2006**, *45*, 10115 – 10125 (Yb–Mn); c) J. A. Kovacs, R. G. Bergman, *J. Am. Chem. Soc.* **1989**, *111*, 1131 – 1133 (W-Zr). No reference to Ni–W systems was found.

[12] a) [($^{i\text{Pr}}$PCP)Ni(OH)]: J. Cámpora, P. Palma, D. del Rio, E. Álvarez, *Organometallics* **2004**, *23*, 1652 – 1655 (d(Ni-O) = 1.865(2)); b) [$^{i\text{Pr}}$PCP)Ni(OMe)]: J. Cámpora, P. Palma, D. del Rio, M. M. Conejo, E. Álvarez, *Organometallics* **2004**, *23*, 5653 – 5655 (d(Ni-O) = 1.855(2)).

[13] V. A. Levina, O. A. Filippov, E. I. Gutsul, N. V. Belkova, L. M. Epstein, A. Lledós, E. S. Shubina, *J. Am. Chem. Soc.* **2010**, *132*, 11234 – 11246.

[14] a) N. V. Belkova, L. M. Epstein, A. I. Krylova, E. G. Faerstein, E. S. Shubina, *Russ. Chem. Bull.* **2007**, *56*, 870 – 874; b) N. Avramovic, J. Hock, O. Blacque, T. Fox, H. W. Schmalle, H. Berke, *J. Organomet. Chem.* **2010**, *695*, 382 – 391.

[15] N. V. Belkova, L. M. Epstein, E. S. Shubina, *Eur. J. Inorg. Chem.* **2010**, 3555 – 3565.

[16] For an example of a side-on bridging H_2 ligand, see: J. P. Collman, J. E. Hutchinson, P. S. Wagenknecht, N. S. Lewis, M. A. Lopez, R. Guilard, *J. Am. Chem. Soc.* **1990**, *112*, 8206 – 8208. For another curious example of a side-on μ_3-H_2 coordination to a Ru_3 triangle, see: G. Süss-Fink, L. Plasseraud, A. Maisse-François, H. Stoeckli-Evans, H. Berke, T. Fox, R. Gautier, J.-Y. Saillard, *J. Organomet. Chem.* **2000**, *609*, 196 – 203. No examples of structures that contain an end-on bridging coordination mode were found.

[17] a) D. W. Stephan, G. Erker, *Angew. Chem.* **2010**, *122*, 50 – 81; *Angew. Chem. Int. Ed.* **2010**, *49*, 46 – 76; b) S. Grimme, H. Kruse, L. Goerigk, G. Erker, *Angew. Chem.* **2010**, *122*, 1444 – 1447; *Angew. Chem. Int. Ed.* **2010**, *49*, 1402 – 1405; c) T. A. Rokob, A. Hamza, A. Stirling, T. I. Soós, I. Pápai, *Angew. Chem.* **2008**, *120*, 2469 – 2472; *Angew. Chem. Int. Ed.* **2008**, *47*, 2435 – 2438.